Development of Simulation Model for Pyroclastic Flows using COMSOL Multiphysics®

Mauro Iacuaniello[1)], Andrea Montanino[1)], Daniela De Gregorio[2)], Giulio Zuccaro[1,2)]
1) Department of Structures for Engineering and Architecture, University of Naples Federico II, Naples, Italy. E-mail: mauro.iacuaniello@unina.it, andrea.montanino@unina.it, giulio.zuccaro@unina.it
2) PLINIVS - LUPT Study Centre, University of Naples Federico II, Via Toledo 402, 80134, Naples, Italy. E-mail: daniela.degregorio@unina.it

Keywords: **Comsol, Mitigation Strategies, Pyroclastic Flows, Vulnerability assessment**

Introduction

The experience of the eruption in Montserrat in 1997 has shown that the resistance of openings of buildings represents a crucial factor in the evaluation of vulnerability to the stresses caused by pyroclastic flows, although the static nature of the building itself is not compromised. The pyroclastic flows are gas-solid mixture which can flow slope down up to reach considerable distances from the point of emission, with a speed that can easily exceed 100km/h (~ 30m/s). The damage caused by the impact on buildings depends on the combination of several factors: the duration of the phenomenon, the temperature of the flow and the pressure produced by the impact. It has emerged the importance of defining a proper numerical model, which fits best the dynamic pressures and temperature ranges associated with a specific scenario at Vesuvius and the Campi Flegrei, defined in the Emergency Plans. This aim is achieved using the multi-physics based finite element method software COMSOL®. In the analysis carried out, variation in various parameters like geometrical characteristics, different materials, input function temperature were studied and are presented in this paper. Also, fluid-structure analyses were carried out, considering the flow as incompressible single-phase fluid and applying the Reynolds Averaged Navier-Stokes (RANS) turbulent model. Another main objective, once the vulnerability has been defined, is identifying some ordinary mitigation strategies which also represent a solution of energy saving.

Pyroclastic Flows

Pyroclastic flows are fast-moving, dense clouds of hot ash and gases. Near the source of the flow, they are probably completely destructive, but as they travel further away from their source they slow down and become colder. Although they could have limited range of action, the effects can be critical because of the combination of mechanical impact and high temperatures on the vertical surfaces of buildings. Studies of buildings that were in the path of pyroclastic flows at Monserrat (1997) indicated that the window and door openings are the first point of weakness. Indeed, if the opening fails allowing flow materials to enter, the resulting fires are likely to destroy the building entirely. In the case of Vesuvius and Campi Flegrei, PFs can cause a lateral pressure impact within a range from 0.5 to 10 kPa and temperatures ranging between 150 and 450°C. In Campi Flegrei, the probable location of the crater is near very densely populated areas (including the western area of Naples). In this case, the impact of PFs would be particularly serious, whereas in the case of Vesuvius a loss of strength of the initial power is expected because of the distance from the crater of densely built areas.

Exposure

In order to define the best mitigation strategies, it has been necessary to arrange some available data about the buildings in the areas that will be evacuated before the eruption (called 'red zones'), gathered up by the P.LIN.V.S. Among these data, the useful for the purpose are the vertical structure, material of frame and shutters. Indeed, there are different technologies of openings used in the different structures both in the Vesuvian and Phlegrean areas, there is a wide diffusion of buildings framed in reinforced concrete with thick infills panels and masonry structures with square blocks in brick or tuff. Besides, there is a widespread diffusion of aluminium and wood windows with UPVC shutters for both the areas (Fig.1, Fig.2). In this study the most studied openings are the windows, which together with the doors represent a weak point of the building envelope during a pyroclastic flow event (Spence et al. 2004). since the dynamic pressure exceeds the characteristic resistance of them, increasing the vulnerability. So, the data about openings have been divided into three groups:

- Size of openings;
- Frame types;
- Shutters types.

Each of these characteristics is important in assessing the vulnerability and so in defining the adequate mitigation measures. Besides, the sizes of openings were recorded in three classes:

- Large windows, whose area is greater than 1,5 m^2;
- Typical windows, whose area range from 0.5 to 1.5 m^2;
- Small windows, whose area is less than 0.5 m^2.

Aluminium windows

The EN AW-6060 alloy is the most widespread extrusion alloy on the European market, thanks to its high hot forming speed. The alloy allows the production of profiles with even complex sections, including cavities and multiple grooves, to bring the design of the extruded part as close as possible to that of the finished product and to minimize intermediate machining. The mechanical model used is Ramberg-Osgood (1) and the characteristics of the alloy are (Table 1):

Table 1 Physical and mechanical properties of aluminium EN-AW 6060

Density	2700 [kg/m^3]
Elastic modulus	70000 [MPa]
Breaking voltage	160 [MPa]
Poisson Coefficient	0.33
Specific heat capacity	900 [J/kgK]

Thermal conductivity	238 [W/mK]
Thermal expansion	3,7 e^{-7} [1/K]

$$\varepsilon = \frac{\sigma}{E} + K\left(\frac{\sigma}{\sigma_y}\right)^{\frac{1}{n}} \quad (1)$$

- σy is the yield strength of the material,
- σ is the value of the stress considered,
- E Young's modulus,
- n exponent of the hardening of the material.

The type of glass commonly used is composed of silica oxide and lime. As defined in the Instructions for the design, execution and control of constructions with structural glass elements, the latter can be considered a homogeneous, isotropic material with linear elastic behaviour at breakage, both tensile and compressive. The characteristics of this type of glass (Table 2) are:

Table 2 Physical and mechanical properties of soda lime glass

Density	2400 [kg/m^3]
Elastic Modulus	71000 [MPa]
Ultimate Tensile Strength	41 [MPa]
Compressive strength	300 [MPa]
Poisson's ratio	0.33
Specific Heat Capacity	800 [J/kgK]
Thermal Conductivity	1 [W/mK]

The technology hypothesized, as the most common, is that of insulating glass, which indicates the set of two or more sheets of equal or variable thickness, separated by a cavity, usually of air. For the analyses, two panes of the same thickness, i.e. (4/5/6) mm. The geometric model used is thermal break window and door frame (Fig. 3).

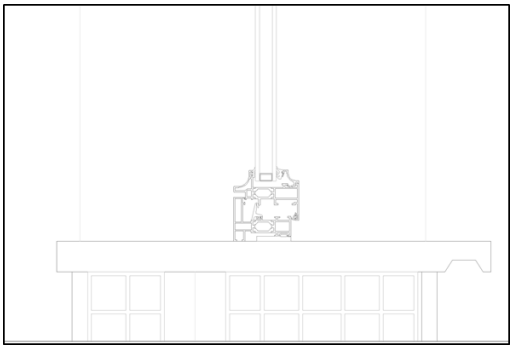

Figure 1 Thermal break aluminium window section

Timber Windows

Another type of material widespread in the Phlegrean and Vesuvian area for the construction of windows and doors is wood. The choice of this material depends mainly on the good thermal insulation characteristics compared to UPVC and aluminum windows and doors. In fact, this choice is economically disadvantageous because wood is certainly a more delicate material compared to PVC and aluminum, as it requires regular maintenance, and because the price of wooden windows and doors is still higher than that of aluminum and PVC.

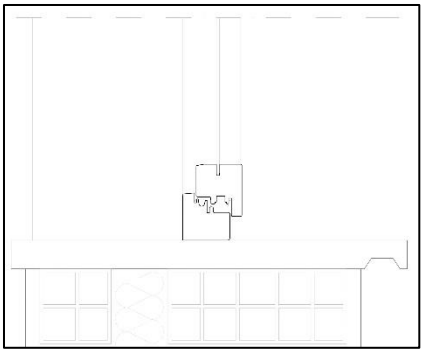

Figure 2 Wood window section

There are several species of wood, belonging to the broadleaf and conifer families, used for the construction of windows and doors:

- chestnut,
- fir,
- pine,
- douglas.

Besides a first hypothesis was to consider the material as a homogeneous and isotropic, whose behavior has been hypothesized linear elastic until breakage. Therefore, the characteristics of the two wood species (Tab. 3, Tab. 4).

Table 3 Physical and mechanical properties of Pine

Density	532 [kg/m^3]
Elastic Modulus	13700 [MPa]
Tensile Strength	85 [MPa]
Compressive Strength	45 [MPa]
Poisson's ratio	0.33

Table 4 Physical and mechanical properties of Chesnut

Density	630[kg/m^3]
Elastic Modulus	114000 [MPa]
Tensile Strength	95 [MPa]
Compressive Strength	51 [MPa]
Poisson's ratio	0.30

Vulnerability Assessment

Mechanical Assessment

To assess the vulnerability of the frames to the pressures expected in both areas, a two-dimensional stationary linear static model (2.1) of the physic Mechanical Structures has been set up for both aluminium and wooden frames. Since the resistance of openings to dynamic pressure depends on several factors of which the most important are the size; therefore, three different heights have been considered for each group of windows, i.e. for the large openings a height of 2.4 m had been considered, for the Typical a height of 1.2 m and for the small a height of 0.8 m has been considered; and for each window size the different thicknesses of the glass have been considered. Furthermore, it has been considered a fixed constraint (2.3) at the base of the wall on which the window is placed (Fig.3). Additionally, it has been considered half section in order to reduce the computational time, assuming a condition of symmetry (2.4) in the upper part of the window.

$$0 = \nabla \cdot (FS)^T + F_V \quad (2.1)$$

$$F_V = I + \nabla_u \quad (2.2)$$

$$u = 0 \quad (2.3)$$
$$u \cdot n = 0 \quad (2.4)$$

In addition, a uniformly distributed load applied (2.5) on the external front has been assumed, in favor of opening, which is linearly variable according to a parameter that has been imposed through a range function.

$$S \cdot \mathrm{n} = F_A \quad (2.5)$$
$$F_A = \frac{F_L}{d} \quad (2.6)$$

Moreover, two different types of Mesh were used, one for the frame and one for the glass sheets. For the aluminum section an extreme finer triangular mesh was constructed, whereas for the glass different "Mapped" Mesh size has been used, in order to take the contact between the two-glass panel into account (Fig.4). For modelling better, the problem and overcoming the convergence problem, it has been necessary to insert a Stop Function in the Solver Configuration, imposing an if condition for the glass:

comp1.StressMax > 40[MPa]

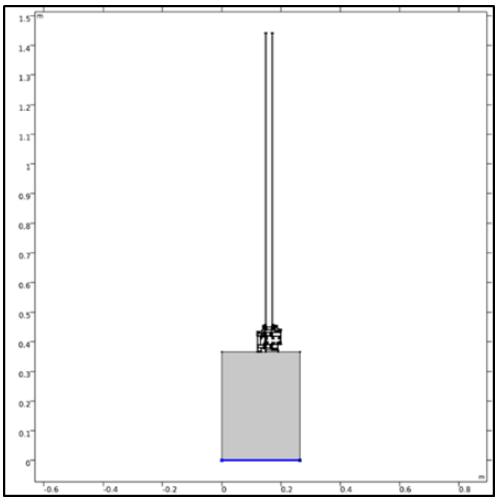

Figure 3 Fixed constraint

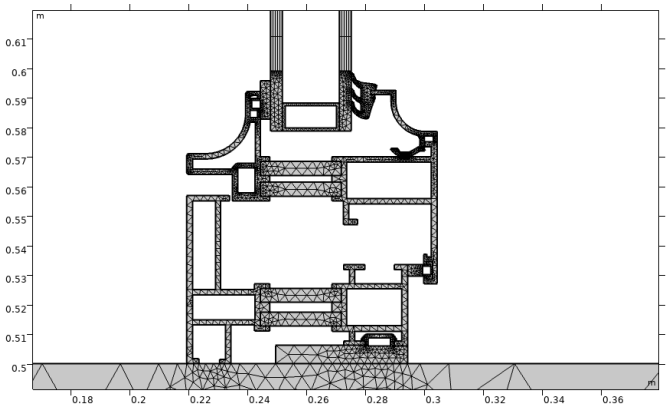

Figure 4 Mesh used for frame and glass

Subsequently, from these first mechanical analyses, the glass of 4 mm of large dimensions, therefore with dimensions equal to 2.4 m of height and 0.6 of thickness, is the most vulnerable because the calculated breaking pressure is equal to 0.6 kPa (Tab.5). This situation is not entirely similar for wooden frames, as the glass of this type is placed inside the frame without the aid of gaskets, so the glass is perfectly embedded in the frame itself (Tab.6). Although the glass in the case of wooden frames may be suitable to withstand the expected pressures, the problem lies in the resistance of the glass to temperature variation**.**

Table 5 Break pressure for aluminum windows

Frame	Aluminium	
Glass	Soda Lime	
Large		
4mm	5mm	6mm
0,6 kPa	1 kPa	1,3 kPa
Typical		
4mm	5mm	6mm
2 kPa	3 kPa	4,3 kPa
Small		
5,3 kPa	8 kPa	10,33 kPa

Table 6 Break pressure for wood window

Frame	Wood	
Glass	Soda Lime	
Large		
4mm	5mm	6mm
1,6 kPa	2,3 kPa	3 kPa
Typical		
4mm	5mm	6mm
4,3 kPa	6,3 kPa	9,3 kPa
Small		
8,6 kPa	14,3 kPa	21,6 kPa

Thermal Assessment

Once the mechanical analysis had been carried out, it was also necessary to set up the thermal analysis. The geometrical model of windows was the same, with a focus on the aluminium one, since there are plastic elements such as the thermal break and the glass seals. In order to tackle this problem two different type of thermal analysis have been accomplished. A 3D heat transfer to assess the thermal shock for the glass and a 2D thermal stress for the entire windows.

Thermal Shock

Thermal shock occurs when a thermal gradient causes different parts of an object to expand in different quantities. This differential expansion can also be understood in terms of stress or deformation (3.1). At some point, this stress may exceed the strength of the material, causing a crack to form. If nothing prevents this crack from propagating through the material, the glazing will lose its structural integrity. Glass objects are particularly vulnerable to failure due to thermal shock, due to their low strength and low thermal conductivity. If the glass is then suddenly exposed to extreme heat, the shock will cause the glass to break.

$$\Delta T = \frac{(\sigma_{TS} * (1-\upsilon))}{E * \alpha} \quad (3.1)$$

where:

- σ_{TS} is the yield strength of the material,
- ν Poisson's ratio,
- E Elastic modulus,
- α coefficient of thermal expansions.

In the case of soda lime glass, the critical temperature is 52 °C. Once the critical temperature is defined, it has been necessary to assess the time to reach it through the heat transfer equation (3.2)

$$\rho C_p\left(\frac{\delta T}{\delta t} + u_{trans} \cdot \nabla T\right) + \nabla \cdot q + q_r = -\alpha T : \frac{dS}{dt} + Q \quad (3.2)$$

where:

- ρ is the density (kg/m^3),
- Cp is the specific heat (J/(kg·K)),
- T is the temperature (K),
- u_{trans} is the speed vector of translational motion (m/s),
- q is the conduction heat flow (W/m^2),
- q_r is the radiation heat flow (W/m^2),
- α is the coefficient of thermal expansion (1/K),
- S is the second Piola-Kirchhoff tensor (Pa)
- Q contains additional heat sources (W/m^2)

To model this problem properly, a time-dependent study was used in the 60 second interval using the range function (0,1,60) s. Moreover, to model the sudden temperature rise, a ramp function (Fig. 5) was applied in the Temperature node, using the following expression:

$$T = 20[degC] + x * rm1(t[1/s]) \quad (3.3)$$

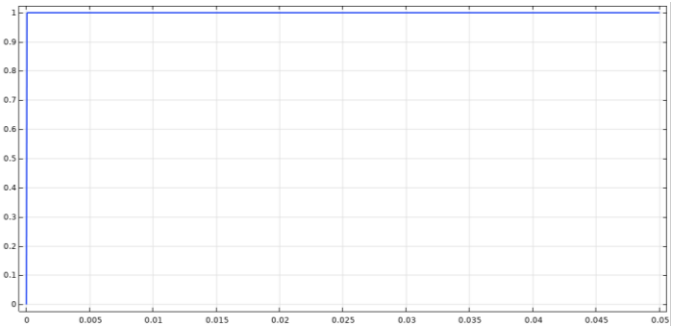

Figure 5 Ramp Function

From this kind of analysis considering an applied temperature of 100 °C, soda-lime glass reaches the critical temperature in the 5-second time interval. (Fig 6). Therefore, soda-lime glass is totally vulnerable to the temperatures expected in the red areas.

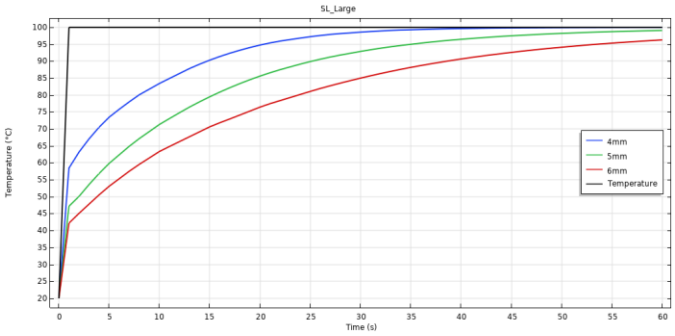

Figure 6 Time of exposure of glass to temperature of 100°C

Aluminium Thermal Resistance

To assess the resistance of the aluminium frame, the stress due to the different temperature was calculated adopting the Thermal Expansion Multiphysics node, which add an internal thermal strain caused by changes in temperature (3.5).

$$\varepsilon_{th} = \alpha(T)(T - T_{ref}) \quad (3.4)$$

$$F_{inel}{}^{-1} \rightarrow F_{th}{}^{-1} F_{inel}{}^{-1}, F_{th} = I + \varepsilon_{th} \quad (3.5)$$

Besides the thermal stress was studied through different function for the temperature. In the first case it was hypothesized a constant temperature from 100°C to 400°C, applied by a ramp function (3.3) throughout the time interval of 1200 s, and the x variable varies from 80 to 380. This model shows that the aluminium can withstand the four different temperature, as there is no breaking-strength of 160 MPa on the frame. Moreover, the second kind of analysis was set up defining the temperature by a Piecewise Function (3.6), where the temperature increases from 20°C to 400°C in the time interval of 240s. The result shows even in this case the frame of the window could withstand; indeed, the frame would only plasticize in some points.

$$T(t) = T_i + T(\Delta t) \quad (3.6)$$

Since this hypothesis cannot perfectly embody the real behaviour of the phenomenon, which is not characterized by only an increase of temperature.

The hypothesized temperature model is an interpolated function (3.7) that presents a sinusoidal variation of temperatures for 240 seconds (Figure 15). The peculiarity of this function lies in the possibility to reach different maximum temperatures by changing the parameter P, indeed if the P is less than one the maximum temperature is around 200°C, while if it is greater than 1, the temperature reaches the 500/600 °C. In the first analysis the maximum temperature was 400°C.

$$T = T_i + sin(T) * t * P \quad (3.7)$$

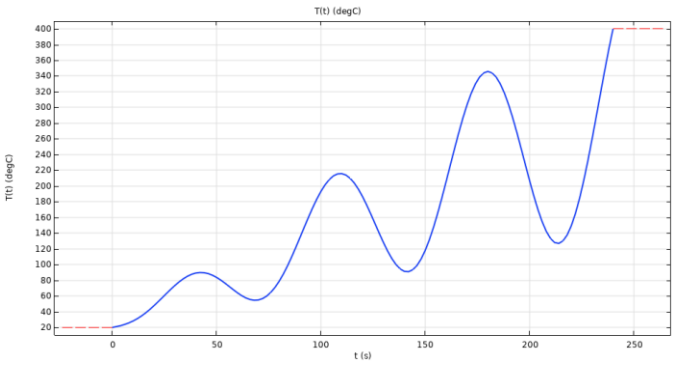

Figure 7 Interpolation Function

These first analyses show that the aluminium frame can resist the high temperatures, and the real issues are the plastic material of thermal break and sealing. Indeed, from the first analysis the polyamide reaches this temperature in a range of 600s in the case of 100°C, while in the case of 200°C, 300°C and 400°C the time is reduced to 50s, 20s and 14s respectively (Fig.8). Besides the EPDM, considering the temperature higher than 100°C, it reaches its critical temperature around the 30 seconds and lower. Finally, if the temperature is described by the interpolated function (3.6), the results show that also in this case the plastic elements are the most vulnerable components of a window; indeed the polyamide reaches its Tg about 100s (Figure 10). At the same time, the EPDM reaches its Tg around 95 s (Figure 11).

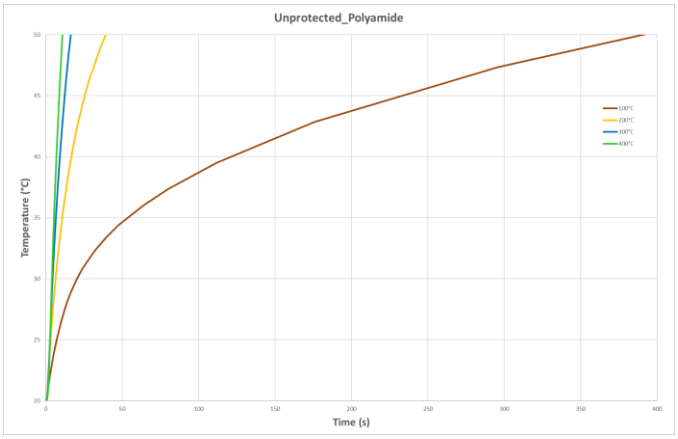

Figure 8 Polyamide exposure time to reach critical temperature

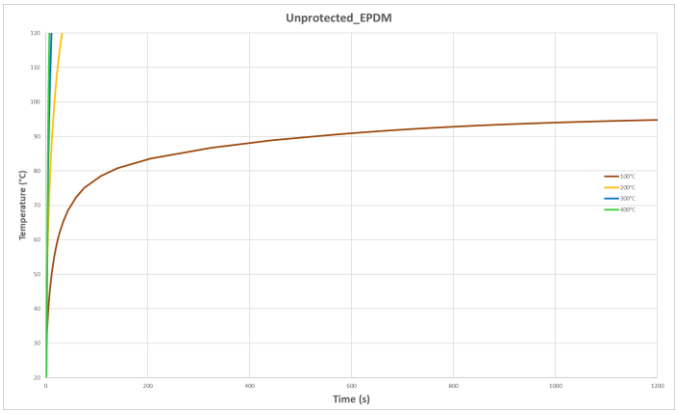

Figure 9 EPDM exposure time to reach critical temperature

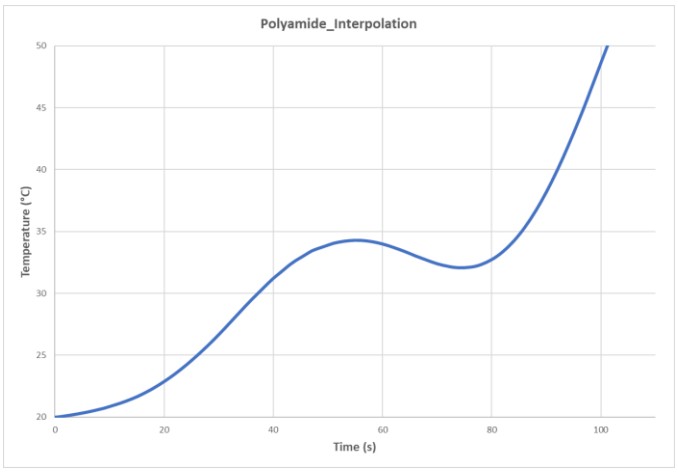

Figure 10 Polyamide exposure time to reach critical temperature

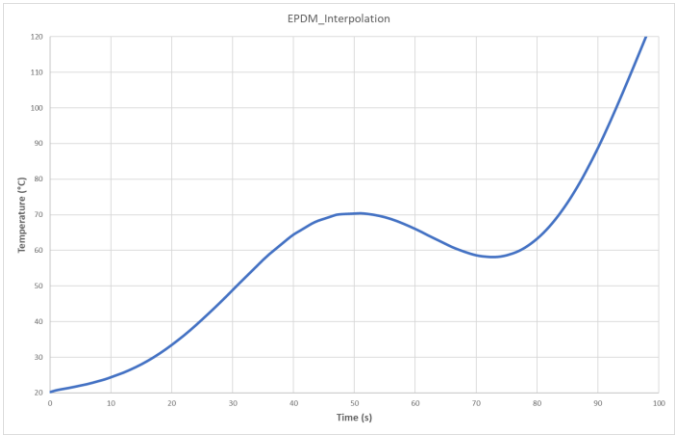

Figure 11 EPDM exposure time to reach critical temperature

Mitigation Strategy

The methodology applied to define the correct mitigation strategy is called incremental innovation. This methodology consists in the improvement (or adaptation) of something that already exists. Therefore, interventions on the different components of the element under consideration. In fact, the interventions foreseen for the window consist, first, in replacing the glass with tempered glass, which has thermal and mechanical characteristics far better than soda lime glass. In addition, to prevent the plastic elements from reaching the glass transition temperature, a 2 cm wooden element is placed in front of the aluminium frame. (Fig. 12).

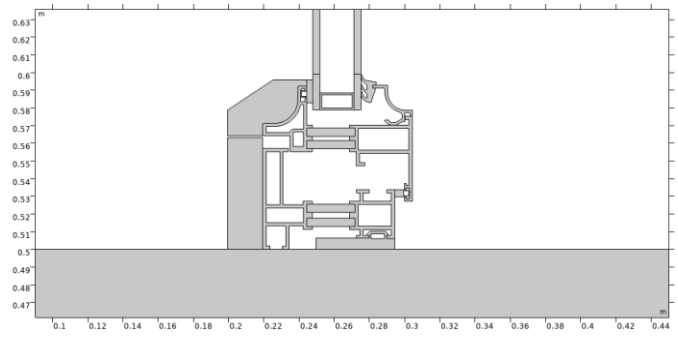

Figure 12 Hypothesis of window

This model has been studied through Therma Expansion Multiphysics node also (3.5). The model, besides, was analysed to the combined actions of pyroclastic flows, in order to fully understand the behaviour. The first step was beginning

from the Heat Transfer time dependent study (3.2). After the simulation, the solution is used in the stationary mechanical study, as initial values of variables solved for and as values of variables not solved for. So, the load which is defined by a range function, is applied on heated window. Besides for overcoming the convergence problem, it has been necessary, also in this study, to insert a Stop Function in the Solver Configuration, imposing an if condition for the glass:

comp1.StressMax > 180[MPa]

The combined analysis shows that the window glass, after the heat transfer to 400°C for 240 seconds, breaks at a pressure of 2.6 kPa (Fig.14). This analysis was also carried out for a window frame with 6mm thick glass, which breaks at four kPa. This strategy, although it represents a good result, cannot be considered as a single intervention. The core of research would identify the strategy that also responds to energy-saving needs; therefore, the shutters have also been analysed through fluid-dynamic models.

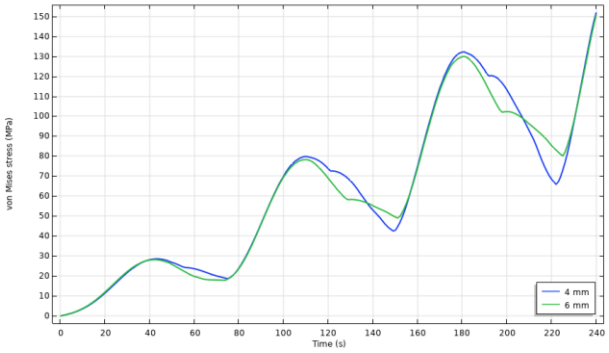

Figure 13 Thermal stress for 4- and 6-millimeter glass

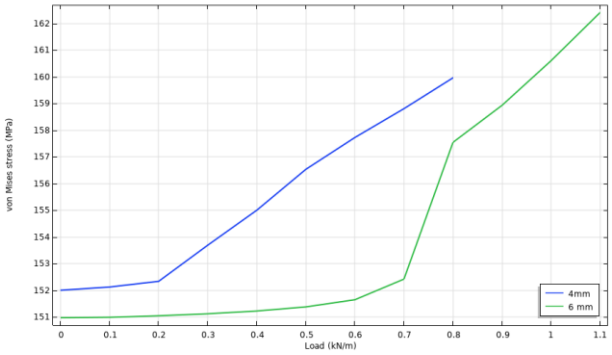

Figure 14 Break load for 4- and 6-millimeter heated glass

Fluid dynamic Assessment

A fluid-dynamic and heat transfer evaluations have been made in the turbulent field, to study the shielding effect of the shutter, changing the inclination of the slots and evaluating if the plastic elements reach the relative critical temperatures. The model uses two different studies: one solving for the turbulent flow around the wall using a Turbulent Flow, k-ε physics interface (4.1), and the other solving for the heat transfer using a Heat Transfer physics interface. The Multiphysics coupling feature Nonisothermal Flow, where the fluid properties depend on temperature.

$$\rho(\mathbf{u_{fluid}} \cdot \nabla)\mathbf{u_{fluid}} = \nabla \cdot [-p\mathbf{I} + \mathbf{K}] + \mathbf{F} \quad (4.1)$$

$$p\nabla \cdot \mathbf{u_{fluid}} = 0 \quad (4.2)$$

$$\mathbf{K} = (\mu + \mu_T)(\nabla u_{fluid} + (\nabla_{u_{fluid}})^T) \quad (4.3)$$

The fluid-flow geometry (Figure 16), is defined as a rectangle where there is a piece of wall with two windows, covered by shutters. The hypotheses are:
- Incompressible fluid,
- Turbulent movement,
- Homogeneous density and speed profile.

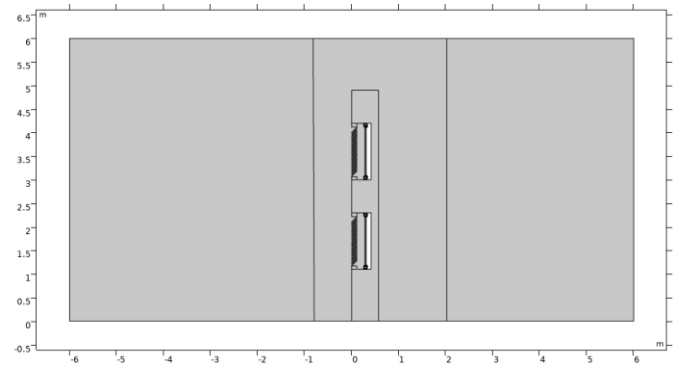

Figure 15 Geometric model for CFD

The physical characteristics of the fluid (Table 7) are:

Table 7 Physical characteristics of pyroclastic flow

Density	2265 [kg/m^3]
Dynamic viscosity	0.001 [Pa * s]
Thermal conductivity	2.2 [W/m * K]
Heat capacity at constant pressure	1255 [J/kg * K]
Ratio of specific heats	1

The pyroclastic flow enters the computational domain at a speed of u = 25 m/s normal to the inlet surface. The floor and the ceiling of the flow domain and surface of the wall are described by wall functions.
The geometric model has been divided into three domains in order to diversify the meshes used. In fact, for flow only domains a mapped mesh of about 2800 elements was used, while in the domain where there is the wall an extra-fine triangular mesh was used, in which there are 92740 elements (Fig.16).

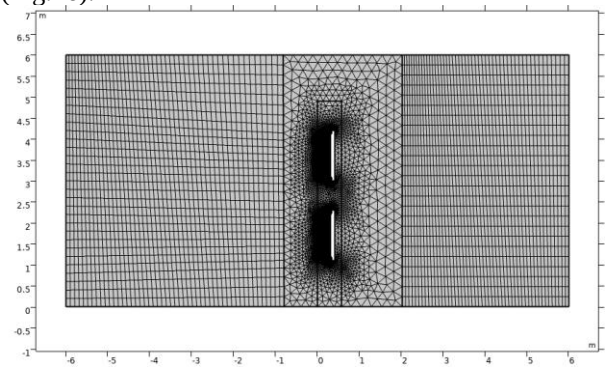

Figure 16 Mesh of the fluid and structures

The first study carried out in the stationary field defined the range of velocity and pressure generated (Fig. 17). Subsequently, the solution obtained from Study 1 was used as initial values of variables solved for the study of Heat Transfer in Solids and Fluids (Fig. 18), defined in the time interval of

240 seconds, and the temperature is expressed through the function (3.7).

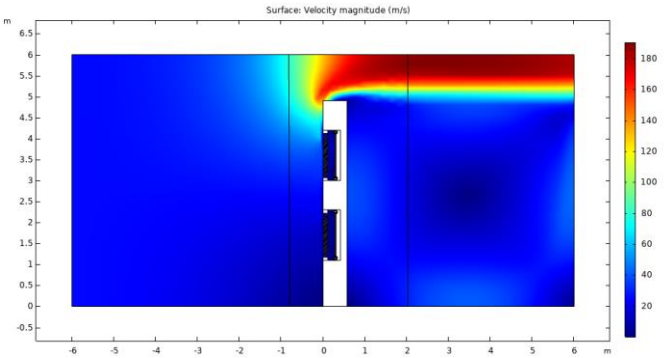

Figure 17 Velocity of fluid

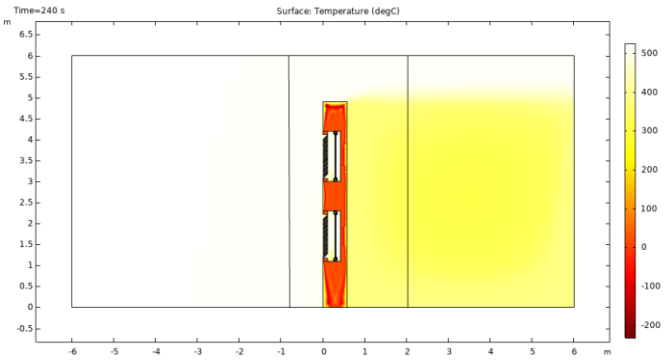

Figure 18 Temperature of elements

The results show that shutters, commonly used, are not suitable for window protection against the flow. The EPDM, in both cases considered, reaches the critical temperature after about 100 seconds. At the same time, polyamide reaches its glass transition temperature after about 120 seconds (Fig. 19). Also, the glass is exposed to the effects of pyroclastic flow, indeed it breaks due to thermal shock after 20 seconds (Fig. 20). Since, the shutters does not fulfil the task so the idea would be to replace the shutters with solid laminated panels that resist both thermal and mechanical stress.

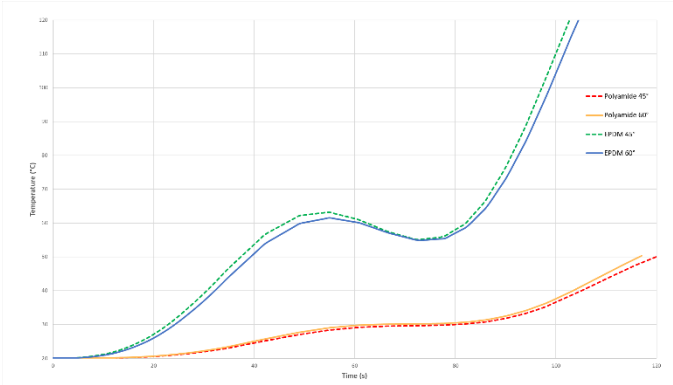

Figure 19 Time of exposure of the plastic elements

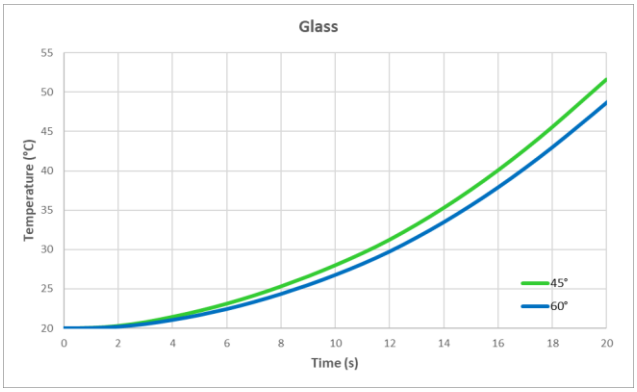

Figure 20 Time of exposure of glass

Conclusions

In this document, we have studied the effects of pyroclastic flows on the openings of a building. The results show that the most significant risk is represented by temperature variation, in fact, the most vulnerable elements: glass, thermal break and seal, once they reach their critical temperature, can no longer perform their function and therefore allow the flow to enter the building and cause considerable damage. Also, the analyses carried out have shown that the proposed measures represent an excellent mitigation strategy; in particular, fluid dynamics analysis has shown that shutters cannot perform any protection. We are therefore studying the possibility of replacing the shutters with a solid stratified panel that can also be used as a curtain wall panel to protect the masonry and can respond to energy-saving requirements. This study will also be carried out in the three-dimensional field to evaluate the effects of pyroclastic flows better.

References

Baxter, P. J., Boyd, R., Cole, P., Neri, A., Spence, R. J. S., and Zuccaro, G. (2005). "The impacts of pyroclastic surges on buildings at the eruption of the Soufrière Hills volcano, Montserrat." Bull. Volcanol., 67(4), 292–313.

Esposti Ongaro, T., Neri, A., Todesco, M., and Macedonio, G. (2001). "Pyroclastic flow hazard assessment at Vesuvius by using numerical modelling. 2: Analysis of flow variables". *Bull. Volcanol., 64, 78-191.*

Spence R.J.S., Baxter P.J., Zuccaro G. (2004a). Building vulnerability and human casualty estimation for a pyroclastic flow: a model and its application to Vesuvius. *J. Volcanol. Geoth. Res.* 133 (2004):321–343, 2004.

Spence R., Zuccaro G., Petrazzuoli S., Baxter P.J., (2004b). The resistance of buildings to pyroclastic flows: theoretical and experimental studies in relation to Vesuvius. *ASCE Nat Hazards* Rev 5:48–50. ISSN: 1527-6988, 2004.

Zuccaro G., Cacace F., Spence R.J.S., Baxter P.J., (2008b). Impact of explosive eruption scenarios at Vesuvius", J Volcanol Geoth Res 178(2008):416–453, 2008.

Zuccaro G. and De Gregorio D., (2013). Time and Space dependency in impact damage evaluation of a sub-Plinian eruption at Mount Vesuvius. Natural Hazard (2013) 68:1399–1423. DOI: 10.1007/s11069-013-0571-8, 2013.

Zuccaro G., De Gregorio D., Baxter P. (2014). Human and Structural Vulnerability to Volcanic Processes. In: P. Papale. (a cura di): J. Shroder, Volcanic Hazards, Risks and Disasters. vol. Chapter 10, p. 261-288, Elsevier, ISBN: 9780123964533.